THE JOURNAL OF PHYSICAL CHEMISTRY B

ARTICLE

pubs.acs.org/JPCB

Copper(II)-Complex Directed Regioselective Mono-*p*-Toluenesulfonylation of Cyclomaltoheptaose at a Primary Hydroxyl Group Position: An NMR and Molecular Dynamics-Aided Design

Ho Law,[†] Juan M. Benito,[‡] José M. García Fernández,[‡] Laszlo Jicsinszky,[§] Serge Crouzy,[∥] and Jacques Defaye*[,†]

[†]Département de Pharmacochimie Moléculaire, Institut de Chimie Moléculaire, CNRS et Université de Grenoble (UMR 5063-FR 2607), BP 53, F-38041 Grenoble, France

[‡]Instituto de Investigaciones Químicas, CSIC-Universidad de Sevilla, Americo Vespucio 49, E-41092 Sevilla, Spain

[§]Cyclolab Research and Development, P.O. Box 435, H-1525 Budapest, Hungary

[∥]CEA, iRSTV, Laboratoire de Chimie et Biologie des Métaux (UMR 5249 CEA-CNRS-UJF), F-38054 Grenoble, France

Supporting Information

ABSTRACT: Interactions between cyclomaltoheptaose (*β*-cyclodextrin, *β*CD) and *p*-toluenesulfonyl chloride (TsCl) were investigated using MD simulations, both in vacuum, approximating the hydrophobic environment of the CD cavity, and with water as a solvent. In both cases, the minimum energy adiabatic paths, and the mean force potentials (MFP) for the insertion of TsCl along a reaction coordinate perpendicular to the CD plane, were calculated for the two possible orientations of TsCl. The results show a preferred entry of TsCl in the CD cavity with the sulfonyl chloride group pointing to the primary hydroxyls rim. In each orientation, two energy minima for the complex are detected in vacuum that reflect the H−H contacts between host and guest observed by NMR spectroscopy (ROESY, NOESY). These separate minima collapsed into a single broader minimum, when the solvent was introduced in the simulations. The resulting association constant between TsCl and *β*CD ($K_a \approx 100\ M^{-1}$) is in good agreement with the NMR results ($K_a = 102 \pm 12\ M^{-1}$) in deuterated water solution at 298 K. Advantage has been taken of the dynamics of the reagent inclusion to set up a one step process involving a transient Cu^{2+} chelate at the secondary hydroxyls rim position for the electrophilic monoactivation of *β*CD at the primary hydroxyls rim using water as solvent.

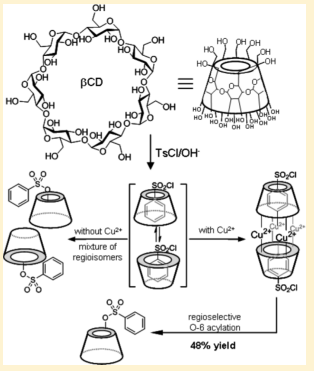

INTRODUCTION

Sulfonic esters of cyclomaltooligosaccharides (cyclodextrins, CDs) are key electrophilic precursors for a variety of modified derivatives with improved physicochemical and supramolecular properties.[1] Among the three possible monosulfonate regioisomers, the 6^I-*O*-sulfonyl derivatives have proven most useful for the controlled attachments of functional elements onto the bucket-shaped structure of CDs via nucleophilic displacement of the sulfonate leaving group. Monosubstitution at the primary hydroxyls rim permits tailoring the interactions with the environment, solvent, or external receptor sites. This can be further exploited for the elaboration of constructs capable of performing specific tasks, including targeted drug delivery and molecular sensing,[2] far beyond the distinctive formation of inclusion complexes with hydrophobic molecules. Unfortunately, with current methods, (O-6) monosulfonylation of cyclodextrins and especially of the more readily accessible representative, namely cyclomaltoheptaose (*β*-cyclodextrin, *β*CD), is not an absolutely selective process. It usually results in mixtures that in addition to the (O-6) monosulfonate contain unreacted starting material, oversubstituted products and regioisomers at secondary hydroxyls positions.[3] Owing to the oligosaccharidic nature of cyclodextrins and the poor stability of sulfonates, purification becomes a problem that represents a bottleneck for further technological development. A methodology for (O-6) monosulfonylation of *β*CD, compatible with high scale preparations, is therefore needed.

The *p*-toluenesulfonyl (tosyl, Ts) functionality is generally preferred for CDs (O-6)-monofunctionalisation,[1,4] although sulfonylation with more hindered arenesulfonates is also effective in the case of cyclomaltooctaose (*γ*CD).[5] Using *p*-toluenesulfonyl chloride (TsCl) as a reagent, 6^I-*O*-tosylation of *β*-cyclodextrin is commonly achieved, either in pyridine[6] or with water[7] as solvent. Acyl transfer from 1-(*p*-toluenesulfonyl)imidazole in water is a valuable alternative procedure.[8] Yields using either of these three approaches are generally in the range 25−40% after very demanding purification steps. Tosyl anhydride in water solution was also claimed[9] to be an efficient high yielding reagent, but in our hands (as with others),[10] this procedure was not reproducible.

Inclusion of *p*-toluenesulfonyl chloride in the cavity of cyclomaltohexaose (αCD) and *β*CD in water solution has been established from concentration-dependent variations in the UV absorption spectra.[4b] This could be exploited to optimize the regioselectivity of the sulfonylation reaction. However, these

Received: February 10, 2011
Published: May 18, 2011

Scheme 1. Schematic Representation of Cyclomaltoheptaose (βCD) and Its Inclusion Complex-Mediated Transformation into the Mono-*O*-Tosyl Derivative

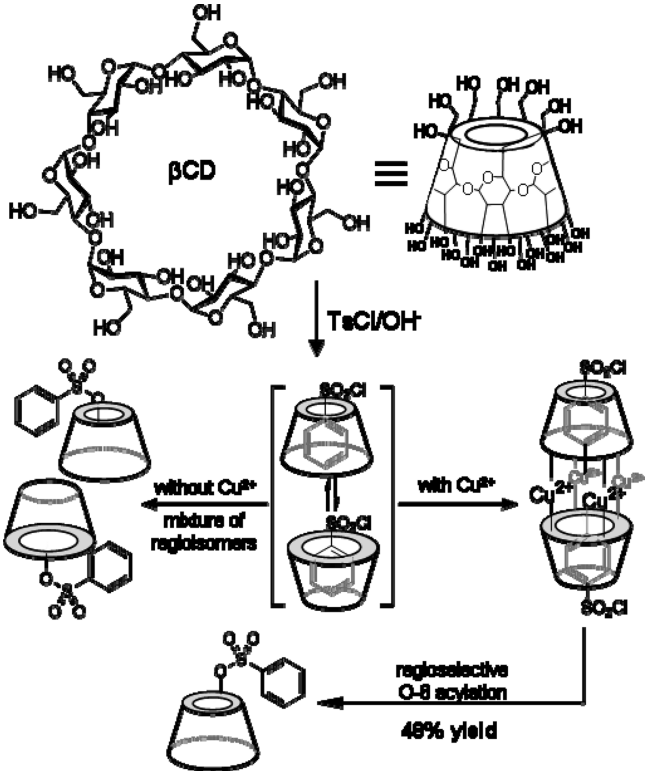

results suffer from some overinterpretation due to misassignement of the sulfonate esterification site.[11] The concept has now been reconsidered using NMR spectroscopy in order to ascertain the geometry of the complex. Molecular modeling simulations have also been carried out to obtain a deeper insight into the dynamics of complex formation. The conclusions of these studies provide a rational explanation for the previously patented[12] regioselective preparation of 6^I-*O*-*p*-toluenesulfonylcyclomaltoheptaose through formation of a ternary complex involving *p*-toluenesulfonyl chloride and the well documented βCD-copper(II) chelate[13] in aqueous alkaline solution (Scheme 1).

EXPERIMENTAL METHODS AND COMPUTATIONAL DETAILS

Materials and Methods. Cyclomaltoheptaose hydrate was from Wacker Chemie (München, Germany, 99% purity) with a water content of 13.8% estimated by loss on drying (100 g scale). *p*-Toluenesulfonyl chloride was purchased from either Sigma Aldrich (>99% purity for laboratory scale experiments, 98% purity for pilot scale experiments) or from Chematek SpA (Lainate-Milano, Italy, for pilot scale experiments; 99.5% purity, ~0.3% $MgCO_3$ and requires removing by filtration from the TsCl/MeCN solution before use). Copper(II) sulfate pentahydrate (>98%) was from Sigma Aldrich. Activated charcoal (purum) was from Fluka. Residual hydration was estimated by Karl Fischer titration and loss on drying.

NMR experiments were recorded with a Bruker Advance 500 MHz instrument. The βCD:TsCl complex association constant (K_a) was determined in D_2O at 298 K by measuring the proton chemical shift changes of solutions of βCD upon addition of increasing amounts of TsCl. In a typical titration experiment, a 3.6 mM solution of host in D_2O was prepared, a 500 μL aliquot was transferred to a 5-mm NMR tube, and the initial NMR spectrum was recorded. A solution of TsCl (3.6 mM) in the previous βCD solution was prepared and stepwise added via a microsyringe to the NMR tube. The ^1H NMR spectrum of each solution was recorded and the chemical shift of the diagnostic signals obtained at 10−12 different host−guest concentration ratios using an iterative least-squares fitting procedure.[14] 1D ROESY and 2D NOESY experiments were recorded using conventional pulse programs. For 1D ROESY, the mixing time was fixed at 0.5 s and the potency was set up to attain a 90° pulse-width of 100 μs. For 2D NOESY, the mixing time was fixed at 0.8 s while TD1 and TD2 were set up to 1024 and 256, respectively. Spectral windows were fixed at 7 ppm in each dimension.

Modeling and Simulations. *Energy Paths.* The βCD molecule was first oriented with its principal axis aligned with the *z*-axis and its center of mass positioned at the origin of the coordinate system. The main axis of the guest (TsCl) was also aligned with the *z*-axis. As for related studies of inclusion complexes with *tert*-butylbenzene[15] or cholesterol,[16] all energy profiles were built by slowly translating the guest along the *z*-axis. The *z*-coordinate *Sz* of the guest sulfur atom was chosen as the reaction coordinate. A few years ago, one of us described the automatic map refinement protocol (AMRP),[17] which allows the automatic refinement of an adiabatic energy map through repeated calls to a program of minimum energy calculation such as CHARMM.[18] The idea is to localize initial energy minima on the path and to minimize neighboring points using the structures of these minima as starting points. After this first path, new energy minima appear, to which the same procedure is applied, until all points on the path have been minimized from the structure of their neighbors. As a result of the AMRP procedure, the path corresponds to local energy minima and the procedure generally has to be repeated several times. Once this "global" minimum energy path has been obtained, the free energy path or potential of mean force (PMF) is calculated using the umbrella sampling technique and WHAM method[19] to recombine and unbias the histograms obtained for all windows along the path (see below). Structure building and MD simulations were carried out using the CHARMM program starting from X-ray structures. Parameters for βCD were the same as described in a previous work[20] and directly transferred from the QUANTA 3.2/CHARMm force field.[21] Charges for TsCl were derived from an ab initio calculation with the program Gaussian 98[22] using RHF theory, the 6-31G* basis set, and the ChelpG algorithm to fit the charges to the electrostatic potential.

General Calculation Settings. Hydrogen atoms were explicitly included, and the SHAKE algorithm[23] was applied to constrain the length of their bond to a heavy atom. Langevin dynamic runs were performed using the Verlet algorithm with 2 fs integration step.

One atom of βCD and its center of mass were almost fixed (harmonic force to keep them close to their original position with force constant 100 kcal/mol/Å^2) to prevent rigid body translation of the system. In addition, O-4 atoms of βCD were subject to harmonic restraints to keep them in the same *xy* plane with a tolerance of 0.8 Å. This range was calculated so that the total restraining force on the initial structure was zero. The end-effect of the previous restraints was to prevent βCD from tilting aside or freely rotating around its principal axis.

Chart 1. Two Protocols Used for the Refinement of Adiabatic (Automatic Map Refinement Protocol, AMRP) and Free Energy Paths (Potential of Mean Force Protocol, PMFP)[a]

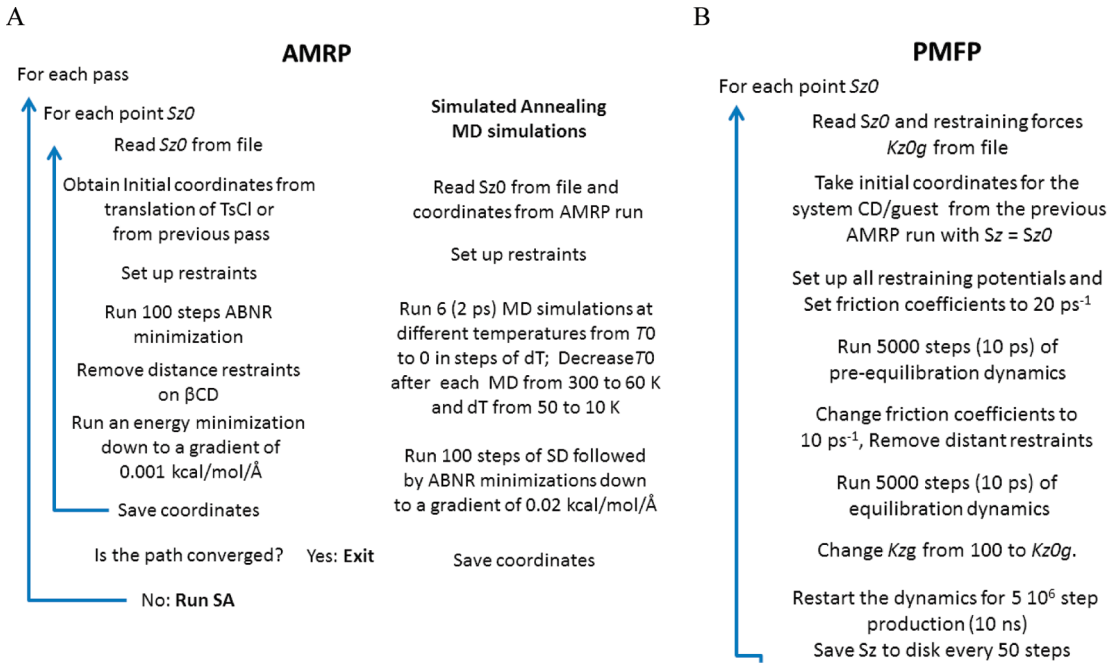

[a] *Sz*0 and *Sz* are the values of the imposed and calculated reaction coordinates respectively. The output of AMRP is a series of structures for all values of *Sz*0 and one adiabatic (potential) energy profile. The output of PMFP is a set of time series of calculated values of *Sz*, one for each value of *Sz*0, which are further binned into histograms and unbiased using WHAM to yield the free energy profile.

All energy profiles were built by slowly translating the guest along the *z*-axis. The *z*-coordinate, *Sz*, of the guest sulfur atom, chosen as the reaction coordinate, was forced to remain inside the *xy* plane with yet another harmonic potential with force constant *Kzg*. The guest was free to move in the *xy* directions. During minimizations, pre-equilibration and equilibration dynamics, *Kzg* was set to 100 kcal/mol/Å^2. It was drastically reduced to values between 6 and 15 kcal/mol/Å^2 during the production stages. During minimization and pre-equilibration, 7 harmonic distance restraints (DR) were applied between O-2 of residue *i* and H of HO-3 of glucose residue *i+1* using a harmonic potential of 10 kcal/mol/Å^2 force constant at long distance and zero energy for distances shorter than 2.5 Å. These restraints helped to preserve the global symmetry of the molecule when VDW contacts were created upon initial introduction of the guest. A friction constant of 20 ps^{-1} was applied on all heavy atoms for Langevin dynamics during pre-equilibration and reduced to 10 ps^{-1} during equilibration and production to maintain a temperature of 300 K.

Vacuum Simulations. Two protocols were followed to calculate the adiabatic paths: in the first one, TsCl was introduced with its methyl group facing the primary hydroxyls side of βCD with *Sz* varying from −20 to +20 Å; in the second one, TsCl was introduced with its methyl group facing the secondary hydroxyl rim of βCD. The sampling of the reaction coordinate which was used was: −20 to −11 Å in steps of 1 Å, −10.5 to +10.5 Å in steps of 0.5 Å, and 11 to 20 Å in steps of 1 Å for a total of 63 points per insertion side. Nonbonded interactions were fully included (a force switch function was used for electrostatics and a shift function for van der Waals interactions with cutoff 50 Å, larger than the maximum interatomic distance in the system). The adiabatic paths were calculated using the AMRP protocol for each point along the paths as detailed in Chart 1A. In vacuum, one pass through AMRP was enough for obtaining the "global" energy paths.

Free energy (potential of mean force) profiles for the inclusion of TsCl into βCD were calculated using the umbrella sampling method.[24] Trajectories were obtained using the protocol detailed in Chart 1B. Values of *Sz* were binned into unbiased histograms using the WHAM program[19] to yield free energy profiles. The good overlapping of the histograms was carefully checked.

Solvent Simulations. βCD and TsCl were solvated with TIP3P water molecules[25] in an orthorhombic box of dimensions ($x \cdot y \cdot z = 20 \times 20 \times 30$ Å). Water molecules with oxygen atom closer than 2.4 Å to any heavy atom (i.e., non-hydrogen atom) were deleted. The particle mesh Ewald method[27] was used to compute electrostatic energies with no cutoff.

Sz was varied from −10 to +10 Å in steps of 0.5 Å. The adiabatic paths were calculated using the AMRP protocol: for each point along the paths. Minimization included the same steps as in the vacuum case except that the final energy minimization was run down to a gradient of 0.01 kcal/mol/Å. Contrary to the vacuum case, however, the first pass through AMRP did not result in a "global" minimum energy path. Far from that, 8 passes through AMRP were necessary before the next pass did not result in a modification to the energy path.

Between two applications of AMRP, we ran simulated annealing (SA) MD simulations on each structure along the path using the protocol explained in Chart 1A. The coordinates of the system were saved ready for the next pass through AMRP. For each adiabatic path, three months CPU time on a recent single processor workstation (3192 MHz, 2 GB RAM) were necessary under the Linux operating system.

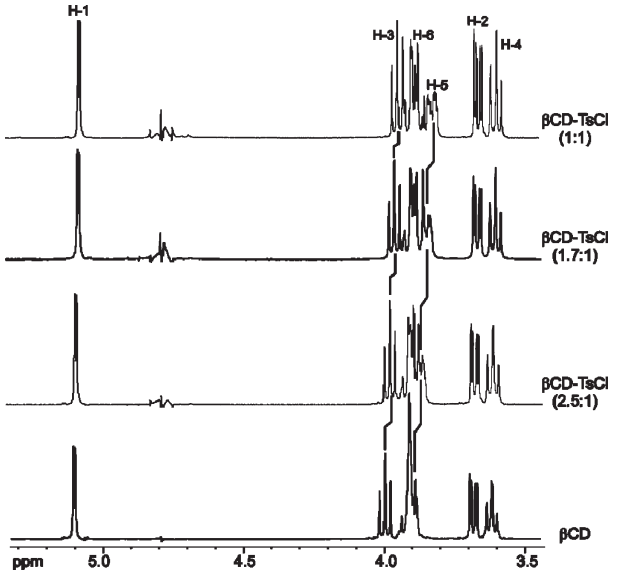

Figure 1. Stacked ^{1}H NMR (500 MHz, D_2O, 298 K) spectra of βCD in the presence of increasing concentrations of *p*-toluenesulfonyl chloride.

Free energy profiles were calculated using the same protocol as described for vacuum except for the fact that the total simulation time was 2 ns per window and coordinates were saved to disk every 5 steps for analysis (200 000 points in each histogram). These histograms both included a large amount of data and showed a nice overlap between perturbation windows which ensures their reliability. The total simulation time (2 ns) per window was chosen so that the maximum free energy difference measured on the PMFs after the two last dynamics (between 1.8 and 2.0 ns, in the present case) was less than 0.2 kcal/mol (and average difference was 0.04 kcal/mol). Each free energy path took 1 month of computer time.

Calculation of Association Constants. The 1 M-standardized association constant, K_a, was obtained by integrating the PMF over the volume accessible to the TsCl molecule, which is close to a cylinder inside the cyclodextrin cavity[27]

$$K_a = N_A \int_z \exp(-\Delta G(z)/k_B T)\, d\tau(z)$$

$$\approx 6 \times 10^{-4} \int_z \exp(-\Delta G(z)/k_B T)\, d\tau(z)$$

where N_A is the Avogadro number and $d\tau(z)$ is the accessible volume expressed in Å^3 in the second equation and which can be written as $\sigma_{ave}(z)\, dz$. The variable $\sigma_{ave}(z)$ is the average cross section of the CD cavity which varies with z.

Tosyl chloride can be viewed as a 6 Å length rod, encompassing 12 slices of 0.5 Å width along the z axis. TsCl is partly inside and partly outside the cavity and, here, $\sigma_{ave}(z)$ has been approximated as the minimum over 12 calculated cross sections inside or outside the cavity

$$\sigma_{ave}(z) = \mathrm{Min}_{slice\ i=1-12}[\sigma_i(z)]$$

In practice, inside the CD cavity, $\sigma_i(z)\, dz$ was calculated with CHARMM as the free accessible volume (with the command "coor volume") on slices of dz = 0.5 Å width and extrapolated outside the cavity as a 5 Å radius cylinder: $\sigma_i(z) = 25\ \pi$. In practice, since ΔG is close to zero in these regions of the PMF, the method of estimating $\sigma_{ave}(z)$ (min or average) and the choice of the extrapolated volume outside the cavity do not modify the results dramatically.

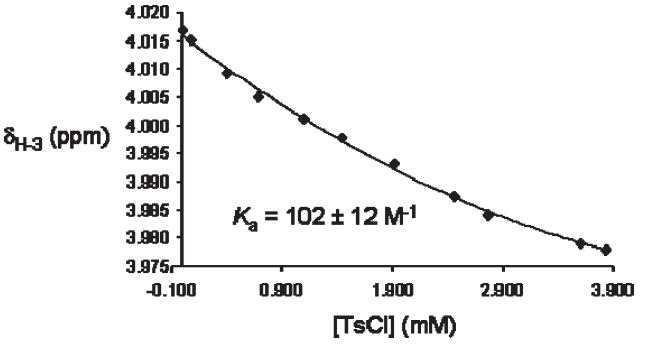

Figure 2. Plot of the chemical shifts of the H-3 resonance of βCD (3.5 mM) vs concentration of TsCl in D_2O at 298 K with indication of the K_a value obtained by nonlinear regression analysis of the corresponding data.

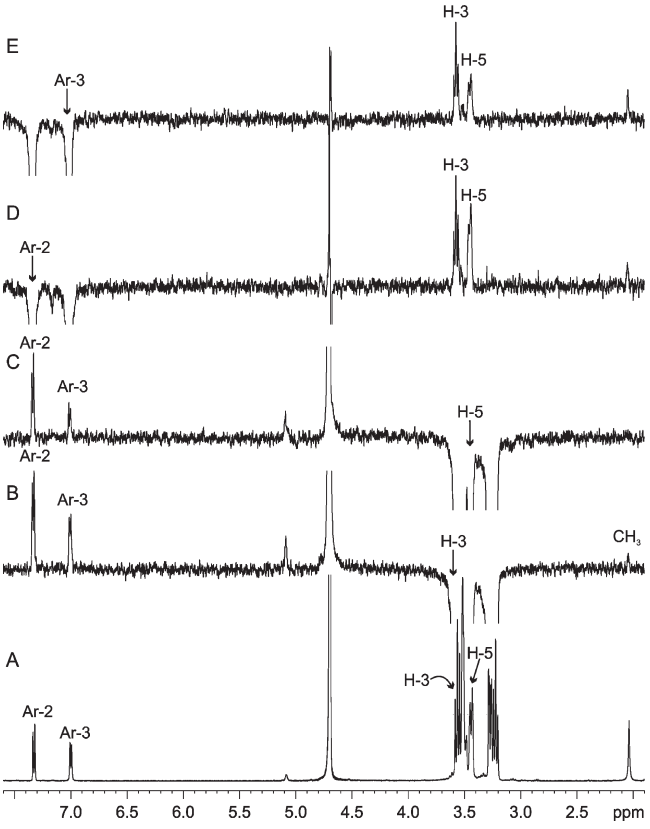

Figure 3. Stacked ^{1}H (A) and 1D ROESY (B-E) NMR spectra of the 1:1 βCD-TsCl complex at 8 mM (500 MHz, D_2O, 278 K). The vertical arrows in B−E indicate the excited proton in each experiment.

Synthesis of 6^I-*O*-*p*-Toluenesulfonylcyclomaltoheptaose. *Bench Scale.* To a suspension of cyclomaltoheptaose hydrate (11.35 g, 10 mmol) in water (500 mL) were successively added $CuSO_4 \cdot 5H_2O$ (7.5 g, 30 mmol) in water (750 mL) and NaOH (10 g, 250 mmol) in water (250 mL). The pH of the reaction mixture was further adjusted to 13.0, monitoring with a pH meter. After 10 min, TsCl (15 g, 79 mmol) in MeCN (100 mL)

dx.doi.org/10.1021/jp2035345 |*J. Phys. Chem. B* 2011, 115, 7524–7532

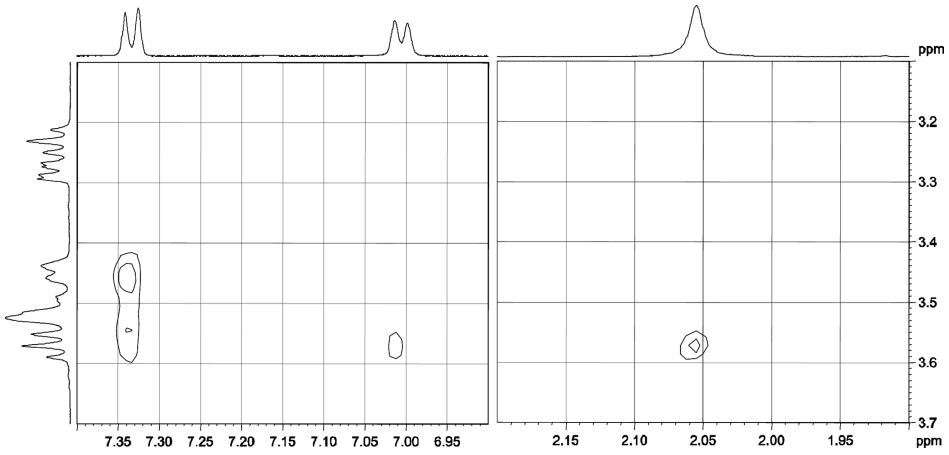

Figure 4. Partial 2D NOESY spectrum of the 1:1 βCD-TsCl complex at 8 mM (500 MHz, D_2O, 278 K) showing diagnostic NOE contacts.

was added dropwise within 1 h. The mixture was stirred for 4.5 h and then neutralized (1 M HCl, 50 mL; pH meter monitoring). The salts were filtered off, and the solution was concentrated by freeze-drying to 2/3 of its original volume. The crystallized solid was washed with acetone (2 × 40 mL) and ether (2 × 30 mL) and air-dried. After two recrystallizations from water, pure 6^1-*O*-tosyl βCD (6.33 g, 48%) was obtained, mp 190−192 °C (dec) (for crystals dried on air),[28] $[\alpha]_D^{20}$ + 122 (*c* 4, Me_2SO); lit.[6] mp 160−162 °C (dec), $[\alpha]_D^{20}$ + 118 (*c* 4, Me_2SO); lit.[7] mp 163−168 °C (dec); lit.[8] $[\alpha]_D^{25}$ + 141 to 146 (Me_2SO, *c* 0.28 to 0.35) (submitters), $[\alpha]_D^{20}$ + 131 (*c* 4, Me_2SO) (checkers); ^{1}H (500 MHz) and ^{13}C (125.7) MHz NMR data identical to those reported.[7] The purity of each preparation was systematically checked by NMR and combustion analysis.

RESULTS AND DISCUSSION

Inclusion Complex Formation of *p*-Toluenesulfonyl Chloride with β-Cyclodextrin. As pointed by Khan et al.,[3] the strength of a cyclodextrin inclusion complex with an electrophilic reagent and the reagent orientation within the cavity could direct the CD-substitution site. ^{1}H NMR spectroscopy has already been widely used to investigate CD-inclusion complexes.[30] Intracomplex formation is expected to induce shifts of the resonances of the H-3 and H-5 protons located within the cavity and from these data the stoichiometry and association constants can be derived. The chemical shifts variations of the 500 MHz ^{1}H NMR spectra of cyclomaltoheptaose upon stepwise addition of *p*-toluenesulfonyl chloride, until reaching a 1:1 molar ratio, are shown in Figure 1. Downfield shifts of H-3 and H-5 are clearly observed, together with some downfield splitting for the H-6,6′ resonances. In contrast, the H-2 and H-4 resonances are only weakly affected. This indicates complexation of the arenesulfonyl halide reagent in the CD cavity.

Although the low solubility of tosyl chloride in water does not permit going beyond the equimolecular host to guest ratio, the corresponding binding isotherm for H-3 in this concentration range (Figure 2) confirms a 1:1 stoichiometry for the complex. The dissociation constant $K_d = 9.8 \times 10^{-3}$ M ($K_a = 102$ M^{-1}), experimentally obtained from the corresponding binding isotherm by an iterative least-squares fitting procedure (see Materials and Methods section) is rather large compared with previous data ($K_d = 1.8 \times 10^{-3}$ M, $K_a = 555$ M^{-1}) obtained from UV experiments at 246 nm.[4b]

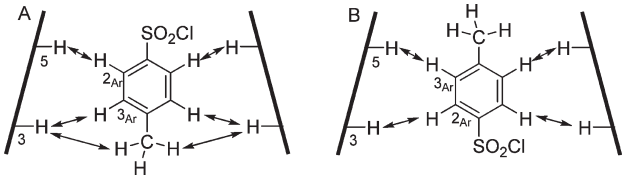

Figure 5. Schematic representation of the two possible orientations of the TsCl molecule in the cavity of βCD in the corresponding inclusion complex.

The geometry of the inclusion complex was explored by 1D ROESY and 2D NOESY experiments at 278 K (Figure 3 and 4, respectively). Irradiation of the H-3 or H-5 resonances in the glucopyranoside subunits showed the existence of strong ROE contacts with both H-2_{Ar} and H-3_{Ar} protons in the aromatic ring. A weaker contact between the H-3 proton and the methyl group in the host was also observed. Conversely, irradiation of H-2_{Ar} and H-3_{Ar} proton resonances indicated their spatial proximity to the H-3 and H-5 protons. Nevertheless, the relative intensity of the ROE signal for the H-5 proton was significantly higher when the H-2_{Ar} resonance was irradiated. The corresponding 2D NOESY spectrum was consistent with these observations. Thus, cross-peaks between H-3/H-2_{Ar}, H-3/H-3_{Ar}, H-3/Me and H-5/H-2_{Ar}resonances were clearly visible.

The above results are consistent with the existence of a fast equilibrium, on the NMR time scale, between the two possible orientations of the guest in the CD cavity (in D_2O solution), i.e., with the sulfonyl chloride group pointing to the primary (Figure 5A) or secondary hydroxyls rim (Figure 5B), but in which the first orientation is favored. An alternative scenario, also compatible with the experimental results, is one in which both orientations are similarly populated. This implies a certain distortion of the βCD macrocycle, resulting in the separation of H-5 and H-3_{Ar} protons, and the concomitant rapprochement of H-3 and H-2_{Ar} protons.

Molecular Dynamics Studies of the *p*-Toluenesulfonyl Chloride/β-Cyclodextrin Inclusion Complex. Molecular mechanics simulations is a well-established method to assess the conformation and dynamics of guest−host inclusion complexes, especially within the cyclodextrin domain.[31] It was of interest to extend the NMR spectroscopy results via this approach so as to ascertain the geometry of binding of *p*-toluenesulfonyl chloride

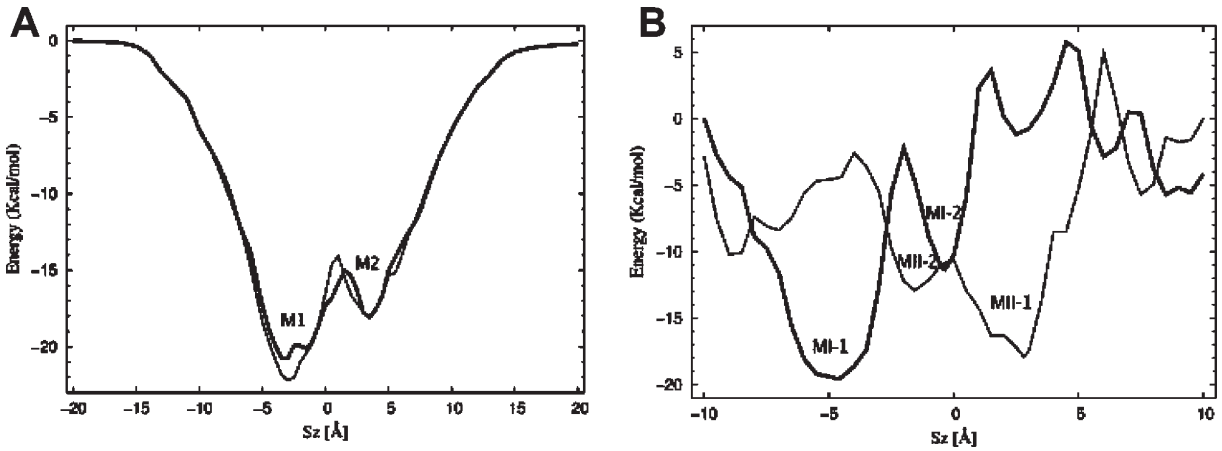

Figure 6. Adiabatic energy profiles for the inclusion of *p*-toluenesulfonyl chloride into βCD. Insertion is done with the *z* coordinate of the S atom of TsCl facing the primary (bold curves MI) or secondary hydroxyl (MII) rims of βCD and simulations are done in vacuum (A) or in water as solvent (B).

in the CD cavity and the side from which the guest enters the cavity. Simulations may also reveal implications in the mechanism of acylation of a primary vs a secondary hydroxyl group.

Structure building and MD simulations were carried out with the CHARMM program using protocols described in the Materials and Methods section. The main axis of the guest (TsCl) and host (βCD) were aligned with the *z*-axis.The *z*-coordinate of the S atom of TsCl (Sz) was chosen as reaction coordinate for TsCl inclusion inside βCD. Initial coordinates for βCD were taken from the X-ray crystallography data of Lindner and Saenger.[32] Those for TsCl were taken from the data of Rigotti et al.[33] The origin of the coordinate system was centered at βCD. TsCl was inserted with its sulfur atom pointing toward both the primary (models MI and Figure 6A) and secondary (models MII and Figure 6B) hydroxyls rim of βCD. Simulations were carried out both in vacuum and in the presence of external solvent (water). Simulations consisted in computing the minimum adiabatic energy and free energy paths for the insertion of TsCl into βCD using reaction coordinate, Sz (see the Experimental Section for details). This method is more accurate than empirical scoring functions used recently in a similar study of the interaction of fluconazole with β-cyclodextrin,[34] but at the expense of much longer simulation times.

The adiabatic energy profiles for the inclusion of *p*-toluenesulfonyl chloride into βCD are shown in Figure 6. Choosing a zero energy level for the TsCl host and CD guest far apart as per usual, we observed two energy minima corresponding to stable complexes (named M1 and M2) in the vacuum. For the water simulation, two additional minima were present. In this latter case, only the two lowest energy minima have been considered. They will be referred to as M*i*-*j* with *i* = I or II denoting the βCD rim and *j* = 1 or 2 denoting the index of the minimum. Characteristic energies of these minima and the *z* coordinate of the TsCl sulfur atom (Sz) are listed in Table 1. The total potential energies are more than 2 orders of magnitude higher than those calculated in vacuum which makes the task of finding minimum energy paths difficult.

The total potential energy is at a minimum when TsCl is inserted into rim 1 of βCD (MI-1) (with Sz = −4.67 Å and relative energy ΔE = −19.6 kcal/mol) and this is followed by a minimum for TsCl inserted into rim 2 of βCD (MII-1) (with Sz = 2.80 Å and *E* = −17.9 kcal/mol). For the vacuum simulation, the situation is opposite with the lowest minimum occurring for TsCl inserted into rim 2 (Sz = −3.0 Å and relative energy *E* = −22.0 kcal/mol) followed by a minimum for insertion into rim 1 (Sz = −3.0 Å and relative energy *E* = −21.1 kcal/mol). Thus, interactions with water can favor different minima as compared with those in vacuum. This is also illustrated by the fact that the interaction energy of TsCl with βCD in the solvent simulation (column 4 of Table 1) is lowest (−16.57 kcal/mol) for the second best energy minimum of MI.

Table 1. Analysis of the Four Minima Found on the Adiabatic Paths for TsCl Insertion into βCD in the Presence of Solvent[a]

minimum	total potential energy (kcal/mol)	TsCl/βCD interaction energy (kcal/mol)	Sz (Å)
MI-1	−4738.4 (−19.6)	−14.05	−4.67
MI-2	−4730.2 (−11.3)	−16.57	−0.36
MII-1	−4737.4 (−17.9)	−15.47	2.80
MII-2	−4732.4 (−12.9)	−10.84	−1.57

[a] Structures in Figure 6. Numbers in parentheses correspond to a choice of a zero energy level for the TsCl host and CD guest far apart from each other.

The structures of the four energy minima are shown in Figure 7. Lowest H−H distances between TsCl and βCD are summarized in Table 2.

Good agreement is found with the experimental NMR results for distances lower than 2.5 Å for H-3/H-2_{Ar} (or H-6_{Ar}), H-3/H-3_{Ar} (or H-5_{Ar}), or H-5/H-2_{Ar} (or H-6_{Ar}).

The free energy profiles (ΔG vs distance between TsCl and the βCD center) showed in Figure 8 give a better picture of the preferred conformations of TsCl inside βCD, including important entropic effects. In vacuum, two minima in the profiles are still seen for the two inclusion sides with a preferred insertion from the primary hydroxyls rim (MI-1). For the case of the MII models, we observe that the two minima have similar energy (−8.3 and −8.1 kcal/mol), whereas for the MI models MI-1 (−9.4 kcal/mol) is largely favored over MI-2 (−7.0 kcal/mol) for insertion in the primary rim. When the solvent is introduced, only one broader minimum is found in the energy curve. However, the main result of a preferred orientation from the primary rim remains. This is confirmed by the values of the association constants

dx.doi.org/10.1021/jp2035345 |*J. Phys. Chem. B* 2011, 115, 7524–7532

(K_a) calculated by integrating the Boltzmann factor-weighted volume of the cavity: $\exp(-\Delta G/k_BT)\ d\tau$ over the well[16,35] and listed in Table 3. Binding to the primary rim is about 1 kcal/mol more favorable than to the secondary hydroxyls rim.

Although small, this difference is most probably significant and the agreement between the theoretical ($86\ M^{-1}$) and experimental ($102\ M^{-1}$) values of K_a is excellent. Results from the vacuum simulation fail to reproduce the experimental results with association constants being more than 100 times larger. In vacuum, the TsCl molecule makes favorable interactions with βCD thus resulting in a high enthalpy stabilization of the complex. In the presence of solvent, this enthalpic stabilization is counterbalanced in part by the desolvation drawback.

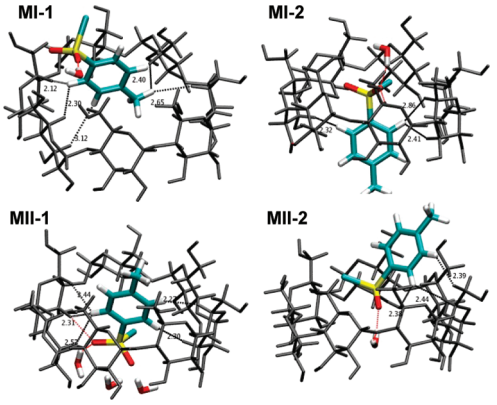

Figure 7. Four minimum energy structures calculated in the presence of solvent for the insertion of TsCl into βCD. Low H−H distances, also seen in NMR experiments and listed in Table 2, are highlighted together with possible hydrogen bonds between TsCl and nearest water molecules. Only water molecules closer than 2 Å from TsCl are shown in tubular representation for better clarity of the pictures.

Table 2. Lowest H−H Distances (Å) between TsCl and βCD Measured from the Four Minimum Energy Structures Shown in Figure 7

minimum	protons	distance (Å)
MI	H-5Ar/H-3	3.12
	H-6Ar/H-3	2.12/2.30
	Me/H-5	2.40/2.65
MI-2	H-2Ar/H-3	2.41/2.86
	H-6Ar/H-3	2.32
MII-1	H-2Ar/H-3	2.30
	H-3Ar/H-5	2.27
	H-6Ar/H-3	2.51/2.87
	H-6Ar/H-5	2.44
MII-2	H-2Ar/H-5	2.38/2.44
	H-3Ar/H-6	2.49

In analyzing these results, one must bear in mind that finding a minimum (or free) energy path along a reaction coordinate during the docking of a ligand to a protein, especially in water, is difficult because of the very large number of local minima (introduced by the solvent degrees of freedom, for instance). Moreover, depending on the choice of the reaction coordinate (here the z-coordinate of the sulfur atom), the energy barriers encountered along the path may vary substantially. Difficulties arise because the energy barriers are in the range of 10 kcal/mol while the total energy of the system is in the range of several thousands kcal/mol. To cope with these difficulties, we used an Automatic Map Refinement Protocol[17] briefly described in the Materials and Methods section (see Chart 1). Although not very efficient in terms of calculation time, the AMRP protocol ensures a soft energy path (no big jumps between points) which then can be used for free energy path calculations. Apart from the small restraints needed to avoid global swinging of the CD (thus possibly presenting its cavity parallel to the reaction coordinate instead of orthogonal) CD was completely flexible in our simulations. Indeed, it has been shown that rigidity or restriction to C_7 symmetry of βCD can lead to "jumps" from one free energy profile to another.[31b]

In summary, insertion of tosyl chloride into the βCD cavity should involve two routes implying both primary and secondary hydroxyl rims of the cyclodextrin cavity. Our calculations show that the preferred orientation for tosyl insertion, corresponding to structures M-I1 and M-II2 in Figures 6 and 7, involves burying of the methyl group. In other words, and as could be expected from its hydrophilic/hydrophobic profile, presentation of the *p*-toluenesulfonyl entity proceeds via its 4-methyl substituent. Insertion via the primary hydroxyls side of βCD is energetically favored, but the alternative route involving entry of the reagent via the secondary hydroxyls side, although less energetically favored is also effective, which explains the incomplete selectivity in the conventional sulfonylation processes.

Cu^{2+}/β-Cyclodextrin Complex Directed C-6 mono-*p*-Toluenesulfonylation. Interaction of "Schardinger dextrins" with Cu^{2+} ions was suspected by Messmer[13a] as long ago as 1927.

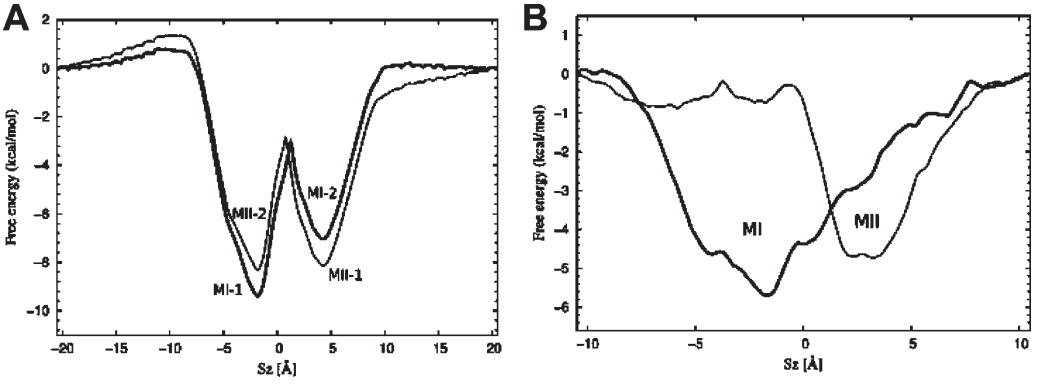

Figure 8. Free energy profiles for the inclusion of *p*-toluenesulfonyl chloride into βCD. Insertion is done with the z coordinate of the S atom of TsCl facing the primary (MI) or secondary (MII) hydroxyls rim of βCD and simulations are done in vacuum (A) or in water as solvent (B).

Table 3. Analysis of the Free Energy Paths for TsCl Inclusion into βCD Primary (MI) and Secondary (MII) Hydroxyls Rim Both in Vacuum (Minima MI-1 and MII-1) and in the Presence of Water As Solvent[a]

	vacuum		solution	
model	ΔG_{min} (kcal/mol)	K_a (M^{-1})/ΔG_{bind} (kcal/mol)	ΔG_{min} (kcal/mol)	K_a (M^{-1})/ΔG_{bind} (kcal/mol)
MI	−9.4 (S_z = −1.85 Å)	29 × 10^3/−6.1	−5.7 (S_z = −1.75 Å)	86/−2.6
MII	−8.3 (S_z = −1.85 Å)	9 × 10^3/−5.4	−4.7 (S_z = 3.15 Å)	19/−1.7

[a] Minimum free energies ΔG_{min} and the corresponding sulfur z-coordinate are given in column 2 and 4. The association constants K_a, calculated as explained in the experimental section,[27] are given in columns 3 and 5.

However confirmation of this observation only came in 1972 when Matsui et al.[13b] were able to isolate a 2:1 Cu^{2+}-βCD complex from its aqueous sodium hydroxide solution. Involvement of four secondary hydroxyl groups of the cyclodextrin core in the complex was subsequently confirmed from both solution[13c−i] and solid state[13j−m] results. In addition, from the large value of their formation[13f] and stability constants[13g] (log$K$ 35.78 ± 0.38 and log β_{Cu2CD} 39.2 ± 0.2 respectively), it was further inferred that such a chelate would be highly stable in the pH range, 12.5−14.3, and likewise involve a deprotonated form of βCD.[36] Based on the results above presented, we subsequently anticipated that these βCD/copper chelates could be ideal scaffolds to control the direction of inclusion of tosyl chloride into the βCD cavity and hence the substitution site.

When a 3-fold excess of copper(II) sulfate in water solution was added to aqueous βCD, followed by addition of sodium hydroxide in order to bring the solution to pH 13, a clear turquoise blue color formed in agreement with the literature, indicating Cu^{2+} complex formation. Dropwise addition of a 9-fold excess of TsCl in acetonitrile at room temperature, standing at the same temperature for a few hours, followed by neutralization of the reaction mixture with aqueous HCl, resulted in salts precipitation. Subsequently, 6^I-*O*-*p*-toluenesulfonylcyclomaltoheptaose was obtained, with yields around 50%, from the supernatant by concentration and recrystallization from water. Of further interest is that copper salts can be easily recycled when the process is scaled up. Large-scale batches amounting to several kg of βCD-monotosylate were obtained with this method (see the Supporting Information).

Conclusions. These results, while introducing a new methodology compatible with large scale access to a key electrophilic precursor for the monofunctionalisation of cyclomaltoheptaose, are a typical example of the possibilities offered by appropriate control of the geometry of reagent inclusion in supramolecular devices such as cyclodextrins. Molecular modeling, in association with NMR spectroscopy, were appropriate tools for establishing the dynamics of the inclusion. The principal originality of MD simulation studies, as compared to previous reports[27,35,36] is the use of detailed path determination (from theories of statistical thermodynamics) to accurately calculate, within the precision of our force field and in parallel with NMR experiments, the binding energy of a small amphiphilic molecule to both sides of βCD in the presence of a solvent. Impeding the pathway leading to inclusion of the reagent through the secondary hydroxyl rim by formation of a metal chelate forces a precise orientation of the TsCl molecule, which results into regioselectivity control. It is advanced that this strategy should not be limited to the present example. Optimization of other transformations involving CD hosts and reactive guests should also benefit from a precise information of the inclusion dynamics obtained by the interplay of computational and spectroscopic techniques in combination with face-selective capping methodologies.

■ ASSOCIATED CONTENT

Supporting Information. Scaled up methodology for the preparation of 6^I-*O*-*p*-toluenesulfonylcyclomaltoheptaose involving the Cu^{2+} supramolecular control of βCD reactivity is detailed. This material is available free of charge via the Internet at http://pubs.acs.org.

■ AUTHOR INFORMATION

Corresponding Author
*E-mail: jacques.defaye@ujf-grenoble.fr.

■ ACKNOWLEDGMENT

This project was supported by the Spanish Ministerio de Ciencia e Innovacion (MICINN, contract No. CTQ2009-14551-C02-01/BQU and CTQ2010-15848), the Junta de Andalucia (P07-FQM2774), the CSIC and the CNRS. We also acknowledge financial support from FEDER funds.

■ REFERENCES

(1) Hattori, K.; Ikeda, H. Modification reactions of cyclodextrins and the chemistry of modified cyclodextrins. In *Cyclodextrins and their complexes*; Dodziuk, H., Ed.; Wiley-VCH: Weinheim, Germany, 2006; pp 31−64.

(2) (a) Lainé, V.; Coste-Sarguet, A.; Gadelle, A.; Defaye, J.; Perly, B.; Djedaïni-Pilard, F. *J. Chem. Soc. Perkin Trans.2* **1995**, 1479–1487. (b) Baussanne, I.; Benito, J. M.; Ortiz Mellet, C.; García Fernández, J. M.; Law, H.; Defaye, J. *Chem. Commun.* **2000**, 1489–1490. (c) Benito, J. M.; Gomez-García, M.; Ortiz Mellet, C.; Baussanne, I.; Defaye, J.; García Fernández, J. M. *J. Am. Chem. Soc.* **2004**, *126*, 10355–10366. (d) Smiljanic, N.; Moreau, V.; Yockot, D.; Benito, J. M.; García Fernández, J. M.; Djedaïni-Pilard, F. *Angew. Chem., Int. Ed.* **2006**, *45*, 5465–5468.

(3) Khan, A. R.; Forgo, P.; Stine, K. J.; D'Souza, V. T. *Chem. Rev.* **1998**, *98*, 1977–1996.

(4) (a) Iwakura, Y.; Uno, K.; Toda, F.; Onozuka, S.; Hattori, K.; Bender, M. L. *J. Am. Chem. Soc.* **1975**, *97*, 4432–4434. (b) Onozuka, S.; Kojima, M.; Hattori, K.; Toda, F. *Bull. Chem. Soc. Jpn.* **1980**, *53*, 3221–3224.

(5) Palin, R.; Grove, S. J. A.; Prosser, A. B.; Zhang, M.-Q. *Tetrahedron Lett.* **2001**, *42*, 8897–8899.

(6) Defaye, J.; Gadelle, A.; Guillier, A.; Darcy, R.; O'Sullivan, T. *Carbohydr. Res.* **1989**, *192*, 251–258. See also ref 7 for improvements.

(7) Brady, B.; Lynam, N.; O'Sullivan, T.; Ahern, C.; Darcy, R. *Org. Synth.* **2000**, *77*, 221–224.

(8) Byun, H.-S.; Zhong, N.; Bittman, R. *Org. Synth.* **2000**, *77*, 225–230.

(9) Zhong, N.; Byun, H.-S.; Bittman, R. *Tetrahedron Lett.* **1998**, *39*, 2919–2920.

(10) Hacket, F.; Simova, S.; Schneider, H.-J. *J. Phys. Org. Chem.* **2001**, *14*, 159–170.

(11) (a) Ueno, A.; Breslow, R. *Tetrahedron Lett.* **1982**, *23*, 3451–3454. (b) Takahashi, K.; Hattori, K.; Toda, F. *Tetrahedron Lett.* **1984**, *25*, 3331–3334.

(12) Defaye, J.; Crouzy, S.; Evrard, N.; Law, H. Regioselective method for preparation of C-6 mono-sulfonated cyclodextrins. PCT Int. Appl. (1999), WO 9961,483 A1, *Chem. Abstr.* 2000, *132*, 24077a.

(13) (a) Messmer, E. *Z. Phys. Chem.* **1927**, *126*, 369–416. (b) Matsui, Y.; Kurita, T.; Date, Y. *Bull. Chem. Soc. Jpn.* **1972**, *45*, 3229. (c) Matsui, Y.; Kurita, T.; Yagi, M.; Okayama, T.; Mochida, K.; Date, Y. *Bull. Chem. Soc. Jpn.* **1975**, *48*, 2187–2191. (d) Mochida, M.; Matsui, Y. *Chem. Lett.* **1976**, 963–966. (e) Matsui, Y.; Kinugawa, K. *Bull. Chem. Soc. Jpn.* **1985**, *58*, 2981–2986. (f) Darj, M.; Malinovski, E. R. *Appl. Spectrosc.* **2002**, *56*, 257–265. (g) Norkus, E.; Grinciene, G.; Vuorinen, T.; Butkus, E.; Vaitkus, R. *Supramol. Chem.* **2003**, *15*, 425–431. (h) Bose, P. K.; Polavarapu, P. L. *Carbohydr. Res.* **2000**, *323*, 63–72. (i) Norkus, E.; Grincienė, G.; Vuorinen, T.; Vaitkus, R. *J. Incl. Phenom. Macrocycl. Chem.* **2004**, *48*, 147–150. (j) Russel, N. R.; McNamara, M. *J. Incl. Phenom. Mol. Recogn. Chem.* **1989**, *7*, 455–460. (k) McNamara, M.; Russel, N. R. *J. Incl. Phenom. Mol. Recogn. Chem.* **1991**, *10*, 485–495. (l) Fuchs, R.; Habermann, N.; Klüfers, P. *Angew. Chem., Int. Ed. Engl.* **1993**, *32*, 852–854. (m) Egyed, O.; Weiszfeiler, V. *Vib. Spectrosc.* **1994**, *7*, 73–77.

(14) The authors kindly thank Dr. C. Hunter for providing the titration isotherm curve fitting program. For a detailed description of the fitting methods and equations, see:(a) Bisson, A. P.; Hunter, C. A.; Morales, J. C.; Young, K. *Chem.—Eur. J.* **1998**, *4*, 845–851. (b) Bisson, A. P.; Carver, F. J.; Eggleston, D. S.; Haltiwanger, R. C.; Hunter, C. A.; Livingston, D. L.; McCabe, J. F.; Rotger, C.; Rowan, A. E. *J. Am. Chem. Soc.* **2000**, *122*, 8856–8868.

(15) Jurcsic, B. S.; Zdravkovski, Z.; French, A. D. *J. Mol. Struct. (Theochem)* **1996**, *366*, 113–117.

(16) Shoup, D.; Szabo, A. *Biophys. J.* **1982**, *40*, 33–39.

(17) Crouzy, S.; Baudry, J.; Smith, J. C.; Roux, B. *J. Comput. Chem.* **1999**, *20*, 1644–1658.

(18) Brooks, B. R.; Bruccoleri, R. E.; Olafson, B. D.; States, D. J.; Swaminathan, S.; Karplus, M. *J. Comput. Chem.* **1983**, *4*, 187–217.

(19) (a) Kumar, S.; Bouzida, D.; Swendsen, R.; Kollman, P.; Rosenberg, J. *J. Comput. Chem.* **1992**, *13*, 1011–1021. (b) Roux, B. *Comput. Phys. Commun.* **1995**, *91*, 275–282.

(20) Goeschl, M.; Crouzy, H.; Chapron, Y. *Eur. Biophys. J.* **1996**, *24*, 300–310.

(21) Momany, F. A.; Rone, R. *J. Comput. Chem.* **1992**, *13*, 888–900.

(22) Frisch, M. J.; Trucks, G. W.; Schlegel, H. B.; Scuseria, G. E.; Robb, M. A.; Cheeseman, J. R.; Montgomery, Jr., J. A.; Vreven, T.; Kudin, K. N.; Burant, J. C.; Millam, J. M.; Iyengar, S. S.; Tomasi, J.; Barone, V.; Mennucci, B.; Cossi, M.; Scalmani, G.; Rega, N.; Petersson, G. A.; Nakatsuji, H.; Hada, M.; Ehara, M.; Toyota, K.; Fukuda, R.; Hasegawa, J.; Ishida, M.; Nakajima, T.; Honda, Y.; Kitao, O.; Nakai, H.; Klene, M.; Li, X.; Knox, J. E.; Hratchian, H. P.; Cross, J. B.; Bakken, V.; Adamo, C.; Jaramillo, J.; Gomperts, R.; Stratmann, R. E.; Yazyev, O.; Austin, A. J.; Cammi, R.; Pomelli, C.; Ochterski, J. W.; Ayala, P. Y.; Morokuma, K.; Voth, G. A.; Salvador, P.; Dannenberg, J. J.; Zakrzewski, V. G.; Dapprich, S.; Daniels, A. D.; Strain, M. C.; Farkas, O.; Malick, D. K.; Rabuck, A. D.; Raghavachari, K.; Foresman, J. B.; Ortiz, J. V.; Cui, Q.; Baboul, A. G.; Clifford, S.; Cioslowski, J.; Stefanov, B. B.; Liu, G.; Liashenko, A.; Piskorz, P.; Komaromi, I.; Martin, R. L.; Fox, D. J.; Keith, T.; Al-Laham, M. A.; Peng, C. Y.; Nanayakkara, A.; Challacombe, M.; Gill, P. M. W.; Johnson, B.; Chen, W.; Wong, M. W.; Gonzalez, C.; and Pople, J. A. Gaussian 98, revision A.11.3; Gaussian, Inc.: Wallingford, CT, 2002.

(23) (a) Ciccotti, G.; Ryckaert, J.-P.; Berendsen, H. J. C. *J. Comput. Phys.* **1977**, *23*, 327–341. (b) Van Gunsteren, W. F.; Berendsen, H. J. C. *Mol. Phys.* **1977**, *34*, 1311–1327.

(24) Torrie, G. M.; Valleau, J. P. *Chem. Phys. Lett.* **1974**, *28*, 578–581.

(25) Jorgensen, W. L.; Chandrasekhar, J.; Madura, J. D.; Impey, R. W.; Klein, M. L. *J. Chem. Phys.* **1983**, *79*, 926–935.

(26) Darden, T.; York, D.; Pedersen, L. G. *J. Chem. Phys.* **1993**, *98*, 10089–10092.

(27) Yu, Y.; Chipot, C.; Cai, W.; Shao, X. *J. Phys. Chem. B* **2006**, *110*, 6372–6378.

(28) Large discrepancies are found in lit. for melting points with the title compound (176−189 °C). This may be ascribed to the method used for mp determination since final decomposition is always involved. Crystallization and drying methods seem also to be considered. A working hypothesis would be that the product may contain autoinclusion compounds involving the tosyl entity (see ref 29).

(29) Djedaïni-Pilard, F.; Gosnat, M.; Steinbruckner, S.; Dalbiez, J. P.; Crini, G.; Perly, B.; Gadelle, A. *Proc. Int. Symp. Cyclodextrins*; Kluwer Academic: Dordrecht, 1999; pp 73−76.

(30) Schneider, H.-J.; Hacket, F.; Rüdiger, V. *Chem. Rev.* **1998**, *98*, 1755–1785.

(31) (a) Lipkowitz, K. B. *Chem. Rev.* **1998**, *98*, 1829–1873.(b) Dodziuk, H. Modeling of CyDs and their complexes. In *Cyclodextrins and their complexes*; Dodziuk, H., Ed.; Wiley-VCH: Weinheim, Germany, 2006; pp 333−355.

(32) Lindner, K.; Saenger, W. *Carbohydr. Res.* **1982**, *99*, 103–115.

(33) Rigotti, B. E.; Rivero, B. E.; Filgueira, R. R. *Z. Naturforsch. B* **1986**, *41*, 1107–1111.

(34) Upadhyay, S. K.; Kumar, G. *Chem. Centr. J.* **2009**, *3*, 9.

(35) Crouzy, S.; Bernèche, S.; Roux, B. *J. Gen. Physiol.* **2001**, *118*, 207–218.

(36) (a) Gaidamauskas, E.; Norkus, E.; Butkus, E.; Crans, D. C.; Grincienė, G. *Carbohydr. Res.* **2009**, *344*, 250–254. (b) Norkus, E. *J. Incl. Phenom. Macrocycl. Chem.* **2009**, *65*, 237–248.

(37) Chen, W.; Chang, C.-E.; Gilson, M. K. *Biophys. J.* **2004**, *87*, 3035–3049.